

An Optimized H5 Hysteresis Current Control with Clamped Diodes in Transformer-less Grid-PV Inverter

1st Sushil Phuyal

Department of Electrical Engineering
Tribhuvan University
Lalitpur, Nepal
076bel047.sushil@pcampus.edu.np

2nd Shashwot Shrestha

Department of Electrical Engineering
Tribhuvan University
Lalitpur, Nepal
076bel043.shashwot@pcampus.edu.np

3rd Swodesh Sharma

Department of Electrical Engineering
Tribhuvan University
Lalitpur, Nepal
076bel048.swodesh@pcampus.edu.np

4th Rachana Subedi

Department of Electrical Engineering
Tribhuvan University
Lalitpur, Nepal
076bel033.rachana@pcampus.edu.np

5th Anil Kumar Panjjiyar

Department of Electrical Engineering
Tribhuvan University
Lalitpur, Nepal
anil.panjiyar@pcampus.edu.np

6th Mukesh Gautam

Electricity Infrastructure & Buildings Division
Pacific Northwest National Laboratory
Richland, Washington, USA
mukesh.gautam@pnnl.gov

Abstract—With the rise of renewable energy penetration in the grid, photovoltaic (PV) panels are connected to the grid via inverters to supply solar energy. Transformer-less grid-tied PV inverters are gaining popularity because of their improved efficiency, reduced size, and lower costs. However, they can induce a path for leakage currents between the PV and the grid part due to the absence of galvanic isolation between them. This leads to serious electromagnetic interference, loss in efficiency and safety concerns. The leakage current is primarily influenced by the nature of the common mode voltage (CMV), which is determined by the switching techniques of the inverter. In this paper, a novel inverter topology of Hysteresis Controlled H5 with Two Clamping Diodes (HCH5-D2) has been derived. The HCH5-D2 topology helps to decouple the AC part (Grid) and DC part (PV) during the freewheeling to make the CMV constant and in turn, reduces the leakage current. Also, the additional diodes help to reduce the voltage spikes generated during the freewheeling period and maintain the CMV at a constant value. Finally, a 2.2kW grid-connected single-phase HCH5-D2 PV inverter system's MATLAB simulation has been presented with better results when compared with a traditional H4 inverter.

Index Terms—Common Mode Voltage, Electromagnetic Interference, HCH5-D2 Topology, Leakage Current, Photovoltaics

I. INTRODUCTION

Distributive Energy Resources (DERs) consisting of a variety of energy types such as solar, wind, and Battery Energy Storage System (BESS) are generally connected to a centralized or islanded power grid. DERs have been widely adopted in both commercial and residential areas [1]. Also, DERs such as solar energy and wind energy are extensively used to complement BESS, enabling the storage of excess energy during low demand and its utilization during high demand [2]. During periods of sufficient sunlight, grid integrated inverters are used to inject or store solar energy by converting DC power into AC and involve a feedback loop [3]. Line frequency

transformers are mostly used in commercial PV inverters to provide galvanic isolation between PV and grid but are often large, heavy, and expensive. Transformer-less inverters (TLI) are being developed to increase efficiency, reduce size, and lower costs [4]. TLIs exhibit higher efficiency due to the absence of losses associated with magnetic coupling, including core and copper losses [5]. However, removing the isolation capability of the transformer requires careful consideration to ensure safety and reliability when connecting solar power directly to the grid [6]. Grounding the PV frame to earth introduces parasitic capacitances between the PV array and the ground [7], which range from 60 nF/kW to 160 nF/kW in normal conditions. This parasitic capacitance forms an LC resonant circuit consisting of a PV array, grid, and converter circuit, allowing unwanted leakage current to flow into the grid, leading to harmonic content, losses, and electromagnetic interference. The German standard VDE0126-1-1 states that leakage currents over 300mA must trigger a break within 0.3 seconds and send a fault signal [8].

The leakage current primarily depends upon the magnitude and nature of CMV. This CMV is the function of switching pattern of the inverter switches. In conventional inverter topologies, the CMV is not constant, as a consequence, this leads to the injection of leakage current to the inverter and to the grid too [9]. There are lots of inverter topologies that use various combinations of switches that makes the CMV constant or DC in nature. Bipolar modulation can maintain constant CMV but due to its bipolar nature the switching losses of the inverter is high where as unipolar modulation is able to reduce the switching losses but cannot maintain constant CMV [10]. So, using H4 topology for leakage reduction with proper efficiency is not possible [11]. Hence, the main aim for controlling the inverter is to suitably mix both modulation techniques as

proposed in HCH5-D2.

Various inverter topologies aim to maintain a constant CMV and improve differential-mode voltage (DMV) performance. Decoupling the AC side from the DC side during freewheeling periods is one effective method for weakening CMV. Topologies such as H5 [12] (DC side decoupling), H6 [13], and HERIC [14] (AC side decoupling) have been developed to reduce CMV fluctuations. However, simple decoupling leads to CMV oscillations at resonant frequencies, making it unstable during freewheeling. Clamping circuits have been introduced to stabilize the CMV during these periods [15]. While previous studies laid the groundwork for transformer-less PV inverters, newer topologies like HCH5-D2 require experimental validation under diverse grid conditions. This paper focuses on common-mode resonant circuit modeling of the HCH5-D2 inverter using the back-to-back source transformation method (Section II), discusses the inverter's modes of operation (Section III), introduces dual control techniques (Section IV), presents simulation results using Matlab/Simulink (Section V), and concludes with key findings (Section VI).

II. PROPOSED HCH5-D2 INVERTER TOPOLOGY

The proposed HCH5-D2 inverter topology uses an additional power switch Q5 compared to H-bridge circuit as displayed in Fig 1. Q5 is placed on the photovoltaic (PV) side, giving this converter a DC-decoupling type of TLI configuration. Q5 is responsible for isolating and disconnecting the DC or PV side of the circuit from the main grid by turning off when necessary thus achieving DC decoupling functionality. Additionally, two clamping diodes are added as shown in Fig.1, whose function is to clamp a CMV to constant magnitude during the freewheeling period. Therefore, these diodes help to reduce the CMV spikes created during the freewheeling period and maintain it to a constant value [16]. Stray capacitive effects between the photovoltaic (PV) array

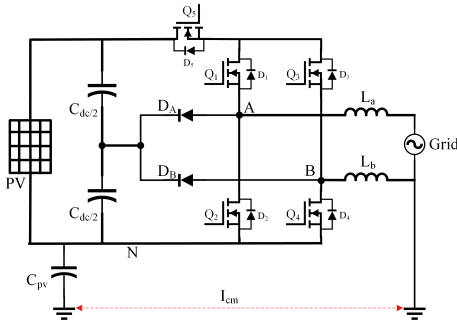


Fig. 1: Main Circuit of HCH5-D2 Inverter Topology

terminals and electrical ground are represented by the parasitic capacitance C_{pv} in the Fig 1. These parasitic capacitances demonstrate the distributed impact of capacitive coupling to stray fields. The pole voltages V_{AN} and V_{BN} at the positive and negative terminals of the PV array are determined by the switching states of the MOSFETs in the converter topology. Specifically, if the upper MOSFETs Q1, Q3, and Q5 are turned

on, the pole voltage will be equal to the DC link voltage V_{DC} . Conversely, if the lower MOSFETs Q2 and Q4 are conducting, the pole voltages will be zero volts.

Likewise Fig.1 illustrates the path of the leakage current I_{cm} , which flows through both the phase and neutral lines of the inverter and to the grid. The modulation strategy employed in this hysteresis current control inverter topology produces a combination of common mode (CM) and differential mode (DM) characteristics when generating the inverter switching signals. The improved CM characteristics' objective is to keep the CMV constant, which reduces the leakage current. Better DM characteristics allow the circuit to generate a multilevel DMV or inverter voltage. As shown in Fig.2a, the circuit in Fig.1 can be resolved into its pole voltages V_{AN} and V_{BN} .

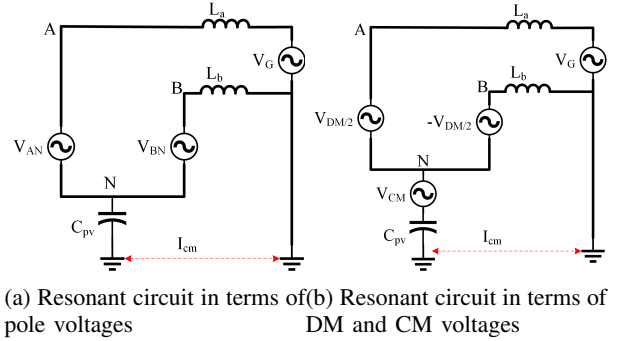


Fig. 2: Resonant circuits of H5 inverter

The average of the pole voltages is known as the CMV. Similarly, the difference between the pole voltages is known as DMV. CMV and DMV can be expressed as.

$$CMV(V_{CM}) = \frac{V_{AN} + V_{BN}}{2} \quad (1)$$

$$DMV(V_{DM}) = V_{AN} - V_{BN} \quad (2)$$

Using the equations (1) and (2), the pole voltages V_{AN} and V_{BN} can be expressed in terms of V_{CM} and V_{DM} as

$$\begin{aligned} V_{AN} &= V_{CM} + \frac{V_{DM}}{2} \\ V_{BN} &= V_{CM} - \frac{V_{DM}}{2} \end{aligned} \quad (3)$$

Likewise, the equivalent circuit is shown in Fig.2a and it can be re-expressed in terms of CM and DM voltage according to (3) as in Fig.2b. A comprehensive analysis is shown below to examine the behavior of leakage current in a transformer-less inverter[17].

A. Conversion of Voltage Sources into Current Sources

The voltage sources which is in series with reactance can be transformed into their respective current sources as displayed in Fig3. Both current sources are operating at very high switching frequencies in the order of kHz whereas grid voltage frequency is just 50 Hz. Therefore, for high frequency analysis, the grid voltage can be neglected.

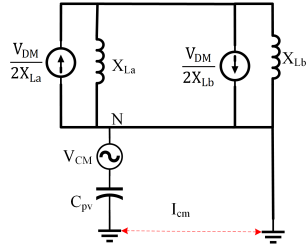


Fig. 3: Resonant circuit of H5 inverter with current sources

The two current sources of Fig.3 in parallel connection can be further resolved into a single current source and with a single voltage source as shown in Fig.4a.

B. Conversion of Current Source into Voltage Source

The single current source in parallel with the reactance in Fig.4a is transferred back to the voltage source with a series reactance, as shown in Fig.4b.

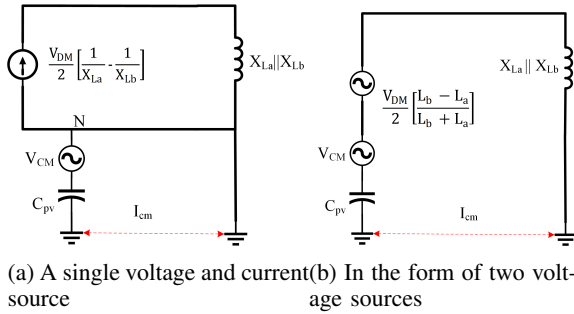


Fig. 4: Resonant circuits of H5 inverter in various voltage and current source configurations

The two voltage sources can be added to form total CMV, V_{tCM} [18]. The final equivalent circuit, to properly describe the nature of CM current is shown in Fig.5

$$V_{tCM} = V_{CM} + \frac{V_{DM}}{2} \left(\frac{L_B - L_A}{L_B + L_A} \right) \quad (4)$$

From (4), it can be understood that when the value of filter inductors L_A and L_B are equal, in both phase and neutral of the grid side, then V_{tCM} will be equal to V_{CM} only with no effect of DM voltage.

C. Leakage Current and Resonant Frequency

From Fig.5, the expression of the leakage current is expressed as

$$I_{CM} = \frac{V_{tCM}}{(X_{LA} || X_{LB}) + X_{C_{PV}}} \quad (5)$$

From (5), it is concluded that the flow and magnitude of leakage current depend upon the value and nature (resonating frequency) of CMV.

The equivalent circuit is called an LC resonant circuit due to the formation of two energy storage elements i.e. equivalent leakage capacitance, C_{eqPV} and equivalent filter inductance,

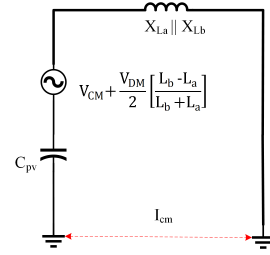


Fig. 5: Simplified resonant circuit of H5 inverter in the form of single common-mode voltage source

$L_{eq} = L_A || L_B$. The LC circuit will oscillate at a resonance frequency given by the equation (6).

$$F_{resonant} = \frac{1}{2\pi} \sqrt{\frac{1}{L_{eq} C_{eqv}}} \quad (6)$$

Equation (5), proves that leakage current depends upon the magnitude as well as the nature of CMV. When the CMV is constant (DC) for each modes of operation, then it will be a DC quantity with a resonant frequency being zero. Therefore, the whole of the denominator of (5) becomes infinity, and hence leakage current tends to zero.

III. MODES OF OPERATION IN PROPOSED HCH5-D2 INVERTER

Unlike a standard H5 topology where the CMV at the freewheeling period is uncertain [12], in the proposed HCH5-D2 topology, the two diodes clamp the pole voltages V_{AN} and V_{BN} to $\frac{V_{DC}}{2}$. The upper diode clamps the upper pole voltage and the lower diode clamps the lower pole voltage to $\frac{V_{DC}}{2}$ during each of the freewheeling modes. The power transfer in the proposed topology is completed in following four modes of operation.

The switching network in Mode 1 allows energy to flow through switches Q1, Q4, and Q5, from the PV to the grid, to get an output of V_{DC} ; the CMV of this mode is equal to $V_{CM} = V_{DC}/2$. For Mode 2, all the switches, except Q1, are turned on, and current freewheels through Q1 and diode D3, isolating the DC side from the AC side. The clamping circuit sets the pole voltage V_{BN} to $V_{DC}/2$ which results in zero output voltage, while V_{CM} remains $V_{DC}/2$. In Mode 3, only switches Q2, Q3, and Q5 are on which transfer energy and generate an output voltage of $-V_{DC}$. Here, the CMV still at $V_{CM} = V_{DC}/2$. Finally, in Mode 4, all switches except Q3 are closed, and the current freewheels through Q3 and diode D1, again decoupling the DC and AC sides. The clamping circuit sets V_{AN} to $V_{DC}/2$, with zero output voltage and the CMV remaining at $V_{DC}/2$. The four modes are illustrated together in Fig. 6.

Based on these four modes, the pole voltages V_{AN} and V_{BN} along with the CM and DM voltages are depicted in the Table I. It is evident that DM voltage maintains unipolar performance i.e. three level voltages $+V_{pv}$, 0, and $-V_{pv}$. Likewise, CM

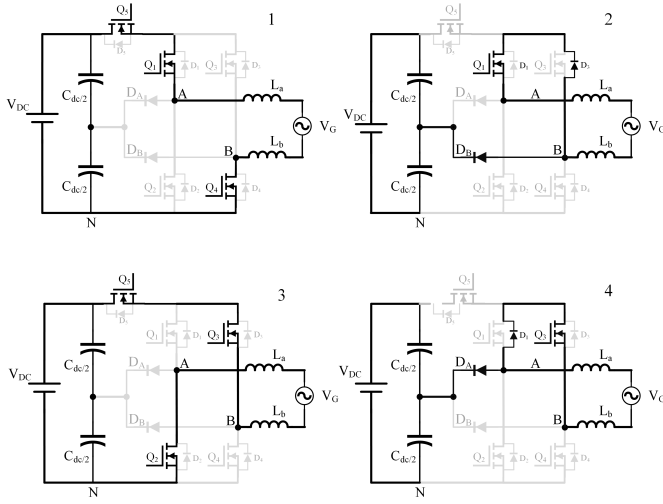


Fig. 6: Different Modes of Operation of HCH5D2

voltage has a constant value in all of the modes. During freewheeling mode, a diode clamps the pole voltages to $V_{pv}/2$. As a result, CM voltage remains constant i.e. $V_{pv}/2$ in all of the modes of operation.

TABLE I: CMV and DMV in different modes of operation of HCH5-D2 topology.

Modes	V_{AN}	V_{BN}	V_{DM}	V_{CM}
(a)	V_{DC}	0	V_{DC}	$V_{DC}/2$
(b)	$V_{DC}/2$	$V_{DC}/2$	0	$V_{DC}/2$
(c)	0	V_{DC}	$-V_{DC}$	$V_{DC}/2$
(d)	$V_{DC}/2$	$V_{DC}/2$	0	$V_{DC}/2$

IV. DUAL LOOP CONTROL STRATEGY FOR THE PROPOSED HCH5-D2 INVETER

The Fig 7 shows the structure for the control strategy that is implemented for HCH5-D2. The system consists of Photo-voltaic Panel, Boost converter with MPPT system, HCH5-D2 inverter, and the EMI filters. Voltage control loop and current control loop are included in the control structure, which are explained in the following subsequent sections.

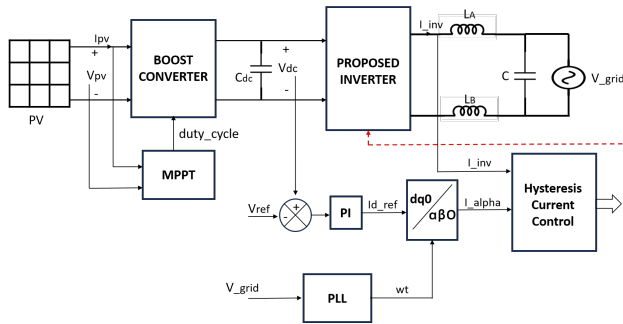


Fig. 7: A control structure diagram for HCH5D2 inverter system.

A. Outer DC Link Voltage Control Loop

To extract maximum power from PV panel, Perturb and Observation (P&O) algorithm is used. The step up boost converter regulates and adjusts the output voltage of the PV panel to match the target voltage, resulting in maximum power production. This loop regulates DC-link voltage at a constant level. Here, the reference voltage value is set as 400 V. By adjusting the reference DC current I_{d_ref} , voltage regulation is achieved. It should be noted that the current I_{d_ref} represents the active component of the reference grid current which corresponds to the active power available at the DC side.

B. Hysteresis Current Control (Inner Grid)

This loop's main function is to synchronize the inverter with the grid i.e., to inject active power to the grid and help to maintain the voltage of DC-link at a fixed value. With the Inverse Park transformation, the alpha component of the current corresponding to I_{d_ref} is used as a reference current in order to set the inverter current to a desirable value. This is achieved from the hysteresis band current controller (HBCC) loop[19]. HBCC compares I_{inv} and I_{alpha} in order to set I_{inv} to a desirable value. The magnitude of the actual current (I_{inv}) is controlled by controlling gating signals of the inverter. Fig.8 shows the variation gate signal in order to maintain the actual current within the tolerance level.

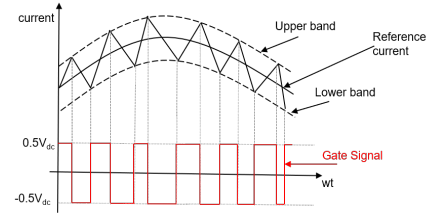


Fig. 8: A Visual Representation of Hysteresis Band Current Control.

V. RESULTS

Proposed HCH5D2 inverter's simulation is performed in MATLAB(Simulink) software with parameters as shown in Table II. The proposed HCH5D2 topology of inverter was analysed and compared with the conventional H4 topology. Grid voltage has been obtained to be in phase with grid current, and hence unity power factor condition is achieved.

TABLE II: Circuit parameters used in MATLAB simulation.

Parameters	Symbol	Value
Grid voltage	v_{grid}	220 Vrms
Input voltage	V_{DC}	400 V
Input capacitors	C_{in1}, C_{in2}	1500 μ F
Output filter inductors	L_1, L_2	4.06 mH
Equivalent parasitic capacitor	C_{PV}	24 nF
MPPT Switching frequency	f_{sw}	20 kHz
Output power	P_{out}	2200 W

A. DC-Link Analysis

With the help of outer DC-link voltage control loop, the simulation model of HCHD-D2 was able to maintain the DC-link voltage at a constant value of 400V as shown in Fig.9a.

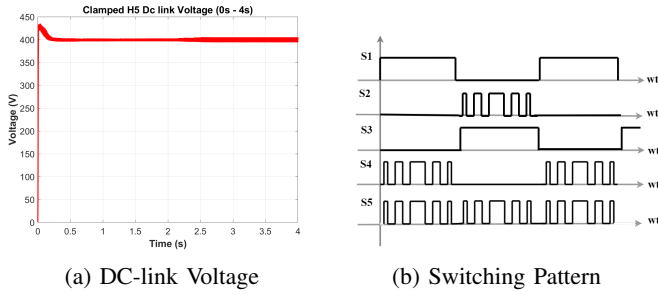


Fig. 9: Simulation results of HCH5-D2 topology.

Likewise, the five different switching signals for the inverter switches, S1-S5 obtained by using Inverse Park transformation of DC reference current and hysteresis band current control are shown in Fig9b.

B. CMV and DMV Analysis

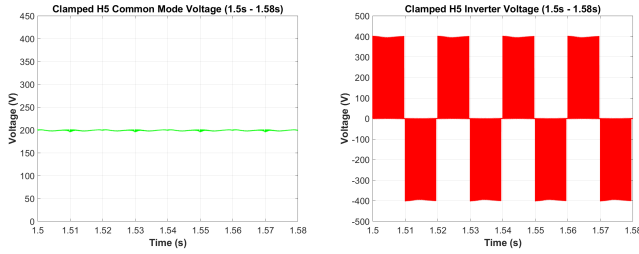


Fig. 10: Simulation results of HCH5-D2 topology.

It can be seen from Fig.10a, the CMV profile is basically constant around $V_{DC}/2$ which is around 200 volts. The upper diode D1 and lower diode d2, during the freewheeling period, were able to clamp the common mode voltage at $V_{DC}/2$ and also reduces the number of spikes. Also, the DMV has unipolar nature as in Fig, 10b, which ensures that the switches of the inverter are subjected to less electrical switching stress which ensures low switching losses.

C. Leakage Current Comparison

The leakage current graphs of conventional H4 inverter and HCH5-D2 inverter are shown in Fig 11a and Fig 11b respectively. Comparing the maximum spikes of leakage current, which exceeded 0.6 A in the conventional H4 topology in Fig 11a.a, this magnitude of current violates the German VDE0126-1-1 standard. Moreover, there's also the possibility of triggering inaccurate signals in several protection devices including circuit breakers. However, in the HCH5-D2, the common mode current is effectively suppressed to a permissible limit by a large instant as compared to that in H4 inverter.

From Table III, it is seen that the leakage current of the HCH5D2 comes to around 1.35mA, which is significantly less than the traditional H4 bridge inverter i.e. 285mA.

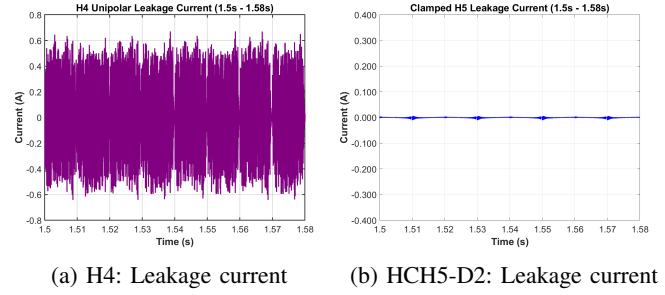


Fig. 11: Comparison of simulation results: Current

TABLE III: Leakage current comparison.

Topology	Leakage Current (RMS)
H4 with unipolar modulation	285 mA
H5	1.35mA

D. Grid Voltage and Current

The waveform of the output current showed the features of a hysteresis band like the gradual rise and decline pattern to ensure that output current follows the reference path. Similarly, the current was also synchronized with the grid voltage apart from the negligible phase lag occurred due to the use of LCL filter circuit. These simultaneous waveforms are presented in the Fig.12a and Fig.12b. Hence, only the active power was injected into the grid.

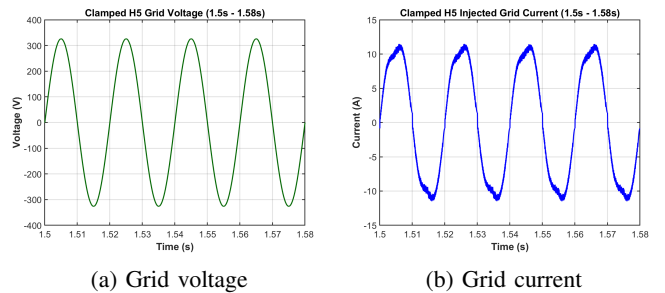


Fig. 12: Simulation results of HCH5-D2 topology.

The Fig13 displays the experimental setup of the proposed HCH5D2 inverter.

VI. CONCLUSION

A 2.2kW grid-connected single phase HCH5-D2 inverter alongside its control strategies are proposed and verified in this paper. The proposed topology was successful in maintaining constant CMV and hence significantly reducing, the leakage current in comparison to conventional H4 topology. The topology also maintains uni-polar characteristics of DMV, which ensures reduced switching stress on the inverter switches

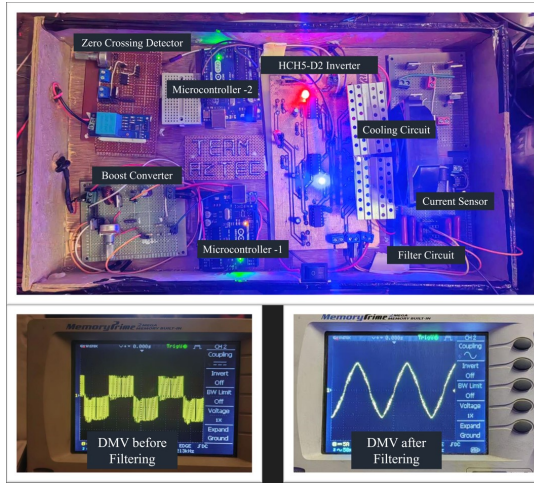


Fig. 13: Experimental setup of HCH5D2 Inverter topology

hence, minimum switching losses. The proposed topology also complies with the German VDE0126–1–1 standard. Additionally, using only five switches and hysteresis band current control this topology ensures simplicity. Hence, HCH5-D2 topology presents a scope to be a good fit for a transformerless PV inverters, typically, in a single phase.

REFERENCES

- [1] A. Awasthi, V. Karthikeyan, V. Das, S. Rajasekar, and A. K. Singh, “Energy storage systems in solar-wind hybrid renewable systems,” *Smart Energy Grid Design for Island Countries: Challenges and Opportunities*, pp. 189–222, 2017.
- [2] S. Phuyal, S. Shrestha, S. Sharma, R. Subedi, and S. Khan, “Predictive load management using IoT and data analytics,” in *International Conference on Artificial Intelligence of Things*. Springer, 2023, pp. 153–168.
- [3] V. R. Vakacharla, K. Gnana, P. Xuwei, B. Narasimharaju, M. Bhukya, A. Banerjee, R. Sharma, and A. K. Rathore, “State-of-the-art power electronics systems for solar-to-grid integration,” *Solar Energy*, vol. 210, pp. 128–148, 2020.
- [4] M. Shayestegan, “Overview of grid-connected two-stage transformer-less inverter design,” *Journal of Modern Power Systems and Clean Energy*, vol. 6, no. 4, pp. 642–655, 2018.
- [5] H. Xiao, “Overview of transformerless photovoltaic grid-connected inverters,” *IEEE Transactions on Power Electronics*, vol. 36, no. 1, pp. 533–548, 2021.
- [6] M. Biswas, S. P. Biswas, M. R. Islam, M. A. Rahman, K. M. Muttaqi, and S. Mueen, “A new transformer-less single-phase photovoltaic inverter to improve the performance of grid-connected solar photovoltaic systems,” *Energies*, vol. 15, no. 22, p. 8398, 2022.
- [7] M. Pourmirasghariyan, S. F. Zarei, and M. Hamzeh, “Dc-system grounding: Existing strategies, performance analysis, functional characteristics, technical challenges,

and selection criteria—a review,” *Electric Power Systems Research*, vol. 206, p. 107769, 2022.

- [8] VDE012611, “Automatic disconnection device between a generator and the public low voltage grid.” 2008.
- [9] M. Calais, V. G. Agelidis, and M. Meinhardt, “Multilevel converters for single-phase grid connected photovoltaic systems: an overview,” *Solar Energy*, vol. 66, no. 5, pp. 325–335, 1999.
- [10] J. Blaacha, R. Aboutni, and A. Aziz, “A comparative study between a unipolar and a bipolar PWM used in inverters for photovoltaic systems,” in *Proceedings of the 2nd International Conference on Electronic Engineering and Renewable Energy Systems: ICEERE 2020, 13-15 April 2020, Saidia, Morocco*. Springer, 2021, pp. 353–360.
- [11] H. Xiao and X. Wang, *Full-Bridge Transformerless PV Grid-Connected Inverters*. Singapore: Springer Singapore, 2021, pp. 35–128.
- [12] M. Victor, F. Greizer, S. Bremicker, and U. Hübler, “Method of converting a direct current voltage from a source of direct current voltage, more specifically from a photovoltaic source of direct current voltage, into a alternating current voltage,” Aug. 12 2008, uS Patent 7,411,802.
- [13] B. Ji, J. Wang, and J. Zhao, “High-efficiency single-phase transformerless PV H6 inverter with hybrid modulation method,” *IEEE Transactions on Industrial Electronics*, vol. 60, no. 5, pp. 2104–2115, 2013.
- [14] K. J. Schmidt H, Siedle C, “Inverter for transforming a DC voltage into an AC current or an ac voltage,” 2003.
- [15] Z. Liao, C. Cao, D. Qiu, and C. Xu, “Single-phase common-ground-type transformerless PV grid-connected inverters,” *IEEE Access*, vol. 7, pp. 63 276–63 287, 2019.
- [16] S. Dhara and V. Somasekhar, “A nine-level transformerless boost inverter with leakage current reduction and fractional direct power transfer capability for pv applications,” *IEEE journal of emerging and selected topics in power electronics*, vol. 10, no. 6, pp. 7938–7949, 2021.
- [17] A. Srivastava and J. Seshadrinath, “Common mode leakage current analysis of 1ϕ grid-tied transformer less H-Bridge PV inverter,” in *2021 International Conference on Sustainable Energy and Future Electric Transportation (SEFET)*, 2021, pp. 1–6.
- [18] A. A. Estévez-Bén, A. Alvarez-Diazcomas, G. Macias-Bobadilla, and J. Rodríguez-Reséndiz, “Leakage current reduction in single-phase grid-connected inverters—a review,” *Applied Sciences*, vol. 10, no. 7, p. 2384, 2020.
- [19] G. Bode and D. Holmes, “Implementation of three level hysteresis current control for a single phase voltage source inverter,” in *2000 IEEE 31st Annual Power Electronics Specialists Conference. Conference Proceedings (Cat. No. 00CH37018)*, vol. 1. IEEE, 2000, pp. 33–38.